Nucleic Acids Research, 1994, Vol. 22, No. 18 3779–3786

Orientations of transfer RNA in the ribosomal A and P sites

Thomas R.Easterwood, François Major[1], Arun Malhotra and Stephen C.Harvey*
Department of Biochemistry and Molecular Genetics, University of Alabama at Birmingham, Birmingham, AL 35294 and [1]National Library of Medicine, National Center for Biotechnology Information, Bethesda, MD 20894, USA

Received May 2, 1994; Revised and Accepted July 11, 1994

ABSTRACT

In protein synthesis, peptide bond formation requires that the tRNA carrying the amino acid (A site tRNA) contact the tRNA carrying the growing peptide chain (P site tRNA) at their 3′ termini. Two models have been proposed for the orientations of two tRNAs as they would be bound to the mRNA in the ribosome. Viewing the tRNA as an upside down L, anticodon loop pointing down, acceptor stem pointing right, and calling this the front view, the R (Rich) model would have the back of the P site tRNA facing the front of the A site tRNA. In the S (Sundaralingam) model the front of the P site tRNA faces the back of the A site tRNA. Models of two tRNAs bound to mRNA as they would be positioned in the ribosomal A and P sites have been created using MC-SYM, a constraint satisfaction search program designed to build nucleic acid structures. The models incorporate information from fluorescence energy transfer experiments and chemical crosslinks. The models that best answer the constraints are of the S variety, with no R conformations produced consistent with the constraints.

INTRODUCTION

Three positions are known to exist in the ribosome for the binding of tRNA (1). The three sites are labeled according to the function of the tRNA at that position. The aminoacyl or A site in the ribosome is where the correct aminoacyl-tRNA is selected and decoding of the mRNA occurs. The aminoacyl-tRNA in this position accepts the growing polypeptide chain from the P site tRNA. The peptidyl or P site on the ribosome is the site in which the tRNA with the polypeptide chain attached is positioned. The existence of a third site, the E site or exit site, has also been elucidated. The presence of a tRNA in the E site has been shown to have a negative allosteric effect on the binding of tRNA to the A site (2). This allosteric effect has been useful in explaining the ability of the ribosome to select the correct tRNA from similar tRNAs thus accounting for the accuracy and speed with which the ribosome interprets the mRNA (3).

The A and P site tRNAs have been shown to bind simultaneously to the message and to the ribosome (4). Distances measured by fluorescence resonance energy transfer (FRET) indicated that the codon–anticodon interaction is simultaneous (4,5). A crosslink between wybutene, the highly modified base at position 37 in the anticodon loop of $tRNA^{Phe}$, and poly U message occurred with both the A and P site tRNAs and did not interfere with translocation of the A site tRNA to the P site (6). A later finding showed that the wybutene crosslinked specifically to the 5′U of the phenylalanine UUU codon (7). The wybutene to 5′U crosslink demonstrated the codon–anticodon interaction by the tRNA is maintained in translocation from A to P site. Recent evidence indicates that the P and E site tRNAs may also maintain simultaneous codon–anticodon interaction (3, and references therein). This may help facilitate the negative allosteric effects found in experiment (2).

Several experimental studies have given a measure of distances between the two tRNAs. The P site tRNA was shown to crosslink to a specific nucleotide in the ribosomal RNA (residue C1400 located near the 3′ end of the 16s rRNA in the small subunit [30S subunit] of the ribosome). The crosslink was characterized by Prince *et al.* (8) and Ofengand *et al.* (9) as a cyclobutane dimer. The crosslink was generated by irradiating with UV light with wavelengths in the range of 300–350nm, a proper range for cyclobutane dimerization. The effects of the dimerization could be reversed by irradiating with ~250nm wavelength light to yield the original reactants. The fact that only tRNAs with pyrimidines in position 34 ($tRNA^{Val}$ and $tRNA^{Ser}$ of *E.coli* and $tRNA^{Val}$ and $tRNA^{Thr}$ of *B.subtilis*) formed crosslinks to C1400 supported the conclusion that cyclobutane dimerization was occurring between rRNA C1400 and tRNA nucleotide 34. The presence of mRNA (in the form of poly GUU) did not interfere with the crosslink. As Prince *et al.* (8) pointed out and modeled in their paper, the cyclobutane dimerization can only occur with the base of C1400 in a stacked position near the P-site tRNA nucleotide 34, implying that the P site tRNA nucleotide 34 is less than 4 Å from C1400.

Gornicki *et al.* (10) and Ciesiolka *et al.* (11) showed that the A site tRNA can also be crosslinked to C1400 using an aryl azide

*To whom correspondence should be addressed

Table I. Constraints used in MC-SYM search procedure

A site tRNA residue	P site tRNA residue	FRET measurements in Å	Range Applied as Constraint in MC-SYM
37	37	24 +/- 4[a]	(20 - 28)
37	16,17	46 +/- 12[a]	(34 - 60)[c]
16,17	37	38 +/- 10[a]	(28 - 48)
16	16,17	35 +/- 9[a]	(26 - 44)
17	16,17	35 +/- 9[a]	(26 - 44)
8	8	26 +/- 4[b]	(22 - 30)

[a]Paulsen *et al.*, JMB (1983) **167**, p411.
[b]Johnson *et al.*, JMB (1982) **156**, p113.
[c]Relaxed Constraint.

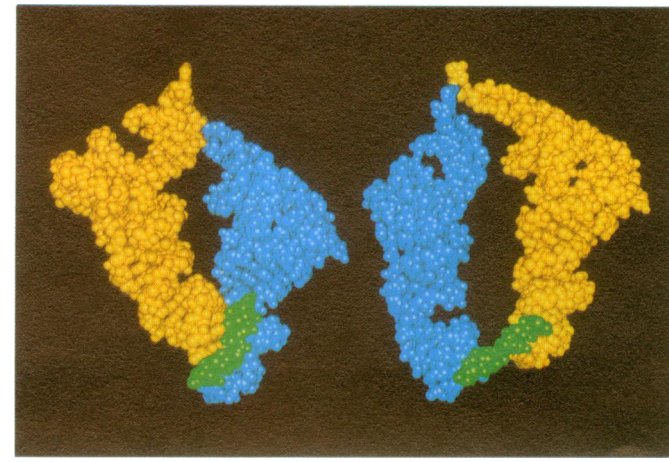

Figure 1. Space filling representation of R model (left) and S model (right). The P site tRNA is yellow, the A site tRNA is blue, with the mRNA in green. The 5′ end of the mRNA is up in the R (left) model, while the 5′ end is to the far right in the S (right) model. Note the close contacts between the acceptor stems (top) and the anticodon loops (bottom). Coordinates for the R and S models are from Lim *et al.*(21).

photoactivatable probe with a tether length of 23−24 Å. The probe was attached to U34 in $tRNA^{Val}$ at position C5 of the base. When the probe was shortened to 18 Å the crosslink yield was decreased four to five fold. This implied that C1400 is 23−24 Å distance from the 5′ nucleotide of the A site anticodon. It is interesting to note that C1400 is the only nucleotide crosslinked from the A site probe (12) and that no direct crosslinks are observed between tRNAs when they are situated in the ribosome (13).

Along with the individual crosslinks, there is evidence that both P and A site tRNAs may be able to crosslink simultaneously to C1400 (12). The experiment involves photodimerization of the P site unmodified $tRNA^{Val}$ to C1400 and the simultaneous chemical crosslinking from the probe on the A site $tRNA^{Val}$ to rRNA. The P site tRNA is crosslinked to C1400 as this dimerization can be cleaved by UV light. The A site probe is simultaneously crosslinked to rRNA, although the exact site of crosslinked rRNA has not been reported. The crosslinked rRNA oligomer has, however, been shown to have a gel migration similar to the rRNA 9mer containing the C1400 crosslink (12).

In addition to the two crosslinks listed above, fluorescence resonance energy transfer (FRET) experiments have given insight into the distances between the tRNAs when they are bound in the A and P sites (14, 15). The fluorescence information summarized in table 1 allows a network of distances to be applied to the two tRNAs. The FRET data and crosslinks provide constraints for model building.

Experiments investigating the replacement of conserved pyrimidines (nucleotides 32 and 33 in the tRNA anticodon loop) with purines has indicated some contacts between the A and P site tRNAs in the ribosome (16). Smith and Yarus used suppressor tRNAs to read through two consecutive stop codons in β-galactosidase mRNA. Nucleotides 32 and 33 in the P site tRNA were changed from pyrimidine to purine and the system was examined for the rate of suppression at the A site by the suppressor tRNA. Smith and Yarus noted a distinct decrease in suppression when nucleotides 32 and 33 were purines. Although these substitutions may be explained by perturbations in the anticodon loop structure (17), the most direct interpretation of this data indicates interactions between A and P site tRNAs. Position 33 in the P site anticodon loop seemed to be especially sensitive to change and is probably in direct contact with the A site (16).

Several models have been proposed previously for the conformation of two tRNAs bound to consecutive mRNA codons as they would be positioned in the ribosomal A and P sites. Fuller and Hodgson (18) first modeled the nucleotide stacking on the 3′ side of the anticodon loop. They showed that 3′ stacking of the anticodon was necessary to allow for loop closure. Fuller and Hodgson also demonstrated the base pairing necessary for codon−anticodon interaction and the probable kink in the message between the two codons to which the tRNAs would be bound. Woese (19) proposed a mechanism where the A site tRNA rotated around the mRNA as it moved into the P site. This reciprocating ratchet mechanism, proposed before the crystal strucure of tRNA was known, was ruled out by the crystal structure, due to the inability of the 3′ ends of the acceptor stems to come close enough to allow transpeptidation. The large molecular motions necessary for rotating the A site tRNA into the P site also did not match the later distance measurements determined by fluorescence.

Two distinct and unequivalent models have been proposed for the conformation of tRNAs in the ribosome. Rich (20) proposed a model depicting the A and P site tRNA positions and discussed the motion necessary for the translocation process. Rich's model (Fig. 1) has the tRNAs upright, acceptor stems at top and directed out of the plane of the page with the anticodon loops down and having the P site tRNA to the left and the A site tRNA to the right. This conformation has subsequently been termed the R model (21). Sundaralingam *et al.* (22) proposed a more detailed model of the A and P site tRNA positions. This model has been termed the S model (21). Using $tRNA^{Phe}$ crystal structures for the A and P site tRNAs Sundaralingam *et al.* explored mRNA phosphodiester torsions between the triplet codons. The S model in figure 1 is depicted with the tRNA acceptor stems directed out of the plane of the page, with the A site tRNA to the left and the P site tRNA slightly elevated and to the right.

Other models similar to the S model have been proposed based on tRNA crystal structure. In these studies either the tRNA anticodons were varied or the mRNA was varied. MacDonald and Rein (23) built S type models using crystal structures of $tRNA^{Phe}$ and $tRNA^{Asp}$ using FRET data (14) for distances

between tRNAs. The tRNA crystal structures were fixed, while the mRNA conformation was allowed to vary in the models. The acceptor stem 3′ ends were positioned so as to allow transpeptidation to occur. Prabahakaran and Harvey (24) also used crystal structures of $tRNA^{Phe}$ to build S type models. Unlike MacDonald and Rein, they allowed the anticodon loop conformations to vary while the six base pairs forming two successive codons in the mRNA were held to a helical form. Prabahakaran and Harvey argued that the true conformation was probably somewhere between the MacDonald and Rein model and the Prabahakaran and Harvey model in that both the tRNA and the mRNA would probably be deformed. These models satisfied the need for simultaneous codon−anticodon interactions and 3′ acceptor stem interactions necessary for peptidyl-transferase activity. Lim *et al.* (21) created both the R and S model in all atom detail using $tRNA^{Phe}$ crystal structures and deforming the mRNA. Lim *et al.* proposed the R model as the best model to explain crosslinking data between the tRNA and ribosome. The crosslinking data implied that the A site tRNA was close to the L7/L12 stalk in the 50S subunit of the ribosome. The direction of mRNA exit from the decoding site was also directed toward the 30S subunit, supporting the R model.

The present study explores the conformational variability of the anticodon loop and the mRNA linkage between the two tRNAs. This is different from previous studies in which either the anticodon loop or the mRNA was held fixed. MC-SYM (25), a constraint satisfaction program based on a tree search methodology, is used to allow the conformational sampling of nucleotides in the anticodon loop and message. Fluorescence data as well as two crosslinks are utilized as distance constraints to narrow the number of possibilities. The resulting structures are all S type models which we believe are in best agreement with the available experimental information.

METHODS

MC-SYM (25, 26, 27) is a computer search program based on constraint satisfaction for building nucleic acid structures. The program uses a tree search algorithm, commonly known as backtracking, to select the appropriate nucleotide conformations and build nucleic acid structures. MC-SYM's search process does not apply a typical search through torsional space. The torsional space is determined by a library of possible structures which are based on existing RNA and DNA structures (27). The library of conformations in MC-SYM are divided into sets (27) that match secondary structural features (e.g. type_A set is one conformation of A type helix, stk_AA is a set of three stacking conformations that vary in backbone torsions and the glycosidic torsion). A computer script specifies which set is to be searched for each nucleotide. One nucleotide conformation is chosen from a set of possible conformations. Each nucleotide chosen represents a node in the search tree. The nucleotide conformation is added to the DNA or RNA structure. If available, constraints derived from experiment are applied to the chosen nucleotide. The program checks the nucleotide against the constraints to determine the conformational fitness of the nucleotide. If the nucleotide conformation is suitable, the conformation for the next nucleotide to be added (the next node along the branch) is selected from its nucleotide set and the process continues. If the conformation is unsuitable in light of the constraints, another conformation is chosen (a new branch issued from the current node is searched) or if all conformations have been tested the program backtracks to the previous nucleotide and the process begins again. The branches under rejected nucleotide nodes are pruned from the search. This process is continued for each nucleotide until a complete structure is built, or the process is halted when a nucleotide set at a specific node is unable to fulfill the required constraints. The structures produced by MC-SYM are not optimized from a molecular energetic standpoint but provide starting structures for refinement and represent the overall conformation of large nucleic acid structures.

Three different kinds of constraints are used in MC-SYM to limit the solutions produced from a search. The first of these, the distance constraint, is used between any pair of atoms. The distance is specified as a range, allowing the inclusion of standard deviation. The second type, the feasible constraint, is applied to two nucleotides. The feasible constraint is used to verify that the distance between two nucleotides can be bridged by a specified number of nucleotides. The feasible constraint does not limit the number of possible solutions, but it does increase the efficiency of the program by 'looking ahead' to ascertain the conformational fitness of the nucleotide. The third type of constraint, the global constraint, is applied to all nucleotides primarily to avoid steric conflicts.

Procedures and constraints used in building the tRNAs have been described previously in Major *et al.* (26). The P site tRNA was built as described (26) with the exception that the closure constraint between residue 33 and 34 was set at 0 to 4 Å. The closure constraint was chosen to maintain the anticodon loop in a configuration comparable to the crystal structure and to allow for easier refinement of the bond between the phosphate at nucleotide 34 and O3′ of nucleotide 33. Conformations in the D loop and T loops were fixed initially to allow a faster search to be performed in the anticodon loop region. The constraints on the tRNAs allow only the anticodon loop to sample nucleotide space, which is most important for the arrangement of the two tRNAs bound to a mRNA. The constraints provided 18 tRNA conformations for the P site tRNA. The polyuridine message which would act as a linkage between the two tRNAs was first paired to the P site tRNA. The sets of nucleotides used to construct this were the sample_pair set (7 Watson−Crick pairing conformations), the stk_AA set (3 base stacking conformations), and type_A set (1 type A helix conformation) for each U residue. A fourth U residue was added in which its connectivity to the 3′ end of the P site codon (UUU) was sampled in all available RNA type sets. The A site tRNA residue 36 was paired to the fourth U residue in the message and the A site tRNA was built in a partially reverse order (i.e.. the anticodon loop and stem were built first and then the D, T, and acceptor stem, in that order). The A site anticodon loop closure (distance from the O3′ of nucleotide 33 to phosphate of nucleotide 34) was also 0 to 4 Å and the D and T loops were fixed. This gave the A site tRNA 18 possible conformations, the same as the P site tRNA.

The constraints between the tRNAs are from FRET data and two crosslinks. FRET information from Paulsen *et al.* (14) and Johnson *et al.* (15), shown in table 1, were applied as distance constraints. At first the A site nucleotide 37 to P site nucleotide 16 and 17 constraint prevented solutions from the search process and this constraint range was eventually relaxed to 34−60 Å. A triangulation method was used to allow the inclusion of the crosslink data. The crosslinks from the A and P site to C1400 can be considered as two sides of a triangle. The greatest distance that can separate the A site tRNA U34 and P site tRNA U34 is 24 + 4 = 28 Å (8, 10, 11). The closest that they may approach

Table II. Root mean squared deviation of MC-SYM created tRNAs from crystal structure

MC-SYM Structures	P site tRNA	A site tRNA
1	3.09	3.15
2	3.09	3.11
3	3.09	3.15
4	3.10	3.12
5	3.10	3.15
6	3.10	3.12
7	3.15	3.11
8	3.11	3.10
9	3.15	3.10
10	3.11	3.10
11	3.15	3.09
12	3.12	3.09
13	3.11	3.09
14	3.10	3.10
15	3.12	3.12
16	3.10	3.10
17	3.30	3.30
18	3.30	3.30
Mean rmsd	3.13	3.13
Std. dev.	0.06	0.06

is 24 − 4 = 20 Å based on the same principle. The distance constraint between the U34, A site tRNA to U34, P site tRNA was therefore set at 24 ± 4 Å. All constraints between the nucleotides were applied to pseudoatoms in the nucleotide conformations. In MC-SYM pseudoatoms are used in place of the purine and pyrimidine base six-sided rings to check steric constraints during the building of a structure. The pseudoatoms were chosen because they best approximate the distance measurements made in experiment (14, 15). The ACCA acceptor ends were not modeled explicitly in the initial search to decrease the search time. Instead, a distance constraint of 50 Å was applied between the ends of the acceptor stems (i.e. between O3′ of nucleotide 72 on each tRNA) to bring the stem ends close enough so that transpeptidation would be possible between the two tRNAs. The 50 Å distance was arrived at in the following way. In MC-SYM the longest nucleotide length is approximately 6.5 Å. Since eight nucleotides are available to bridge the gap between the 3′ end of the acceptor stem (the ACCA from the P site tRNA and the ACCA from the A site tRNA), theoretically $8 \times 6.5 = 52$ Å can be spanned between the acceptor stems. After the search process the ACCA acceptor ends were built by MC-SYM to bring the O3′ of nucleotides 76 on the A and P site tRNAs together.

RESULTS

A list of the root mean square deviation from crystal structure (28) is shown in table 2 for the eighteen P and A site MC-SYM tRNA models. The tRNAs are unrefined and maintain the global L conformation of standard tRNAs. All of the MC-SYM structures maintain a 3′ stacked anticodon and do not include the ACCA 3′ acceptor ends. The eighteen P and A site tRNAs give $18^2 = 324$ possible combinations.

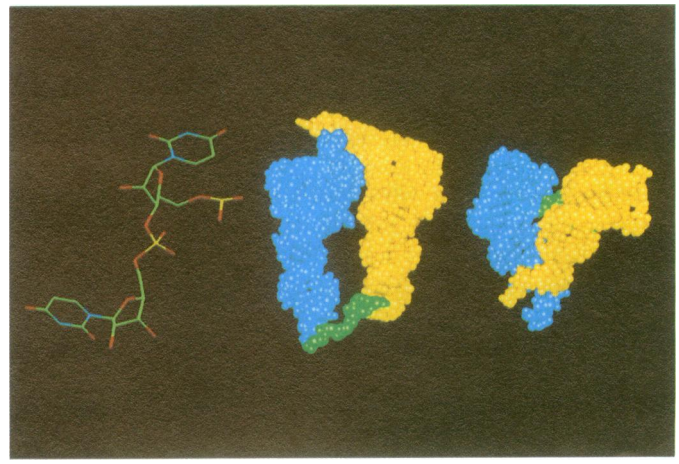

Figure 2. Conformations tagged 384−211. (left) A stick diagram of the 384−211 dinucleotide mRNA linkage between the A and P site tRNA as determined by MC-SYM. (center) A van der Waals representation of the resulting tRNAs with the acceptor stems directed out of the plane of the page showing the S conformation of the model. (right) A top view of the 384−211 model showing the orientation of the A and P site acceptor stems relative to each other and the close approach of the A and P site O3′ ends. In the van der Waals representations, the P site tRNA is in yellow, the A site tRNA is blue, and mRNA in green. The tag denotes the nucleotide conformational numbers from the MC-SYM library used in the dinucleotide linkage structure.

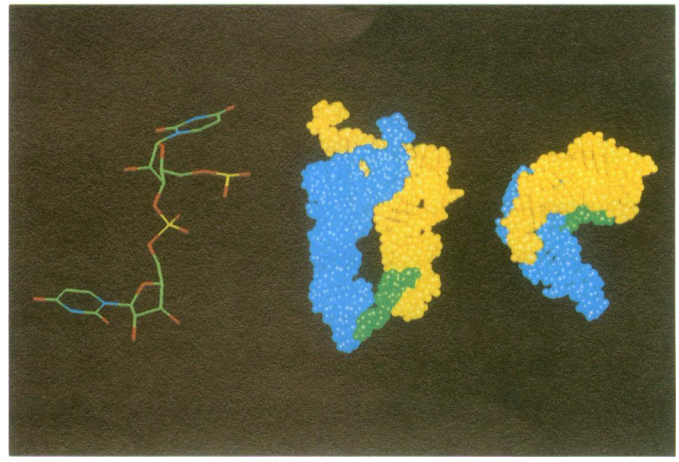

Figure 3. Conformations tagged 93−211. (left) A stick diagram of the 93−211 dinucleotide mRNA linkage between the A and P site tRNA as determined by MC-SYM. (center) A van der Waals representation of the resulting tRNAs with the acceptor stems directed out of the plane of the page showing the S conformation of the model. (right) A top view of the 93−211 model has the P site acceptor stem across the T stem/loop of the A site tRNA. In the van der Waals representations, the P site tRNA is in yellow, the A site tRNA is blue, and mRNA in green. The tag denotes the nucleotide conformational numbers from the MC-SYM library used in the dinucleotide linkage structure.

Six total conformations of tRNAs and mRNA were found to satisfy the FRET distances and crosslink constraints. These six can be divided into two groups, with three conformations in each group. The differences between the two groups are based on the mRNA linkage conformation, specifically the nucleotide conformation chosen by MC-SYM for nucleotide number three in the mRNA. The dinucleotide conformations (nucleotides 3 and

Table III. Torsions angles in nucleotides 3 and 4 of the mRNA, which is the linkage region between the first and second codons

Model *	A	B	C	D	E
χ_3	-175	-151	-151	-169	-169
β_3	180	169	172	174	-115
γ_3	54	72	57	57	-143
δ_3	82	82	80	84	83
ε_3	-142	-142	-158	-132	-163
ζ_3	-158	-158	-80	113	-70
α_4	180	180	-67	-56	-60
β_4	104	104	173	164	175

*Values are given for 5 different models: A: S model from present work, with SYM conformations 384 and 211 for the nucleotides 3 and 4. B: S model from the present work, with MC-SYM conformations 93 and 211. C: Model of Prabahakaran and Harvey (24). D: S model of Lim *et al.* (21). E: R model of Lim *et al.* (21). Standard IUPAC notation is used to identify torsion angles (31).

Table IV. Measurements made on the Lim *et al.* all atom models corresponding to FRET measurements

A site tRNA residue	P site tRNA residue	Lim et al **S** model measurement in Å	Lim et al **R** model measurement in Å
37	37	22	13
37	16,17	63, 66	54, 55
16,17	37	39, 42	39, 44
16	16,17	47, 53	49, 52
17	16,17	51, 56	57, 59
8	8	38	37

(Measurements on the R and S models were made between N9 in purine residues and N1 in pyrimidine residues. Values were rounded down to nearest whole number.)

4 in the mRNA) involved in the linkage between the codons are shown in figures 2 and 3. These dinucleotide conformations are tagged with their MC-SYM conformational numbers, 384−211 and 93−211. The tags denote the 5′−3′ conformational number of the MC-SYM nucleotides used in the dinucleotide linkage between the codons. Most of the variability in this linkage is located in the backbone torsions, as shown in table 3. The sugars maintain a 3′ endo conformation in the linkage. The space filling conformation tagged 384−211 in figure 2 has the back of the A site tRNA facing the front of the P site and is an S type model. The space filling conformation tagged 93−211 in figure 3 has the back of the A site tRNA facing the 'inside corner' of the P site tRNA and is also of the S variety. The resulting structures shown in figures 2 and 3 have not been refined. The conformation tagged 93−211 gave three solutions, representing three combinations of anticodon loops from the P and A sites. The 93−211 conformation used one P site tRNA conformation and three A site tRNA conformations. All of the variability in the A site tRNA anticodon loop is located in nucleotides 33 and 34. Similarly, the 384−211 conformation also gave three solutions in which one tRNA conformation was used in the P site and three tRNA conformations were used in the A site. The variability in the A site anticodon loop for the 384−211 solution was located in the wobble base, nucleotide 34. The variability in the backbone atom positions between the three 93−211 conformations was 0.05 to 0.12 Å rmsd, whereas the 384−211 backbone atom positions varied by 0.04 to 0.05 Å rmsd. The angle between tRNAs in the MC-SYM models are shown by the top views in figures 2 and 3. The 384−211 model has an angle of approximately 45° between the tRNAs. The 384−211 model also allows the closest approach of the ACCA acceptor 3′ ends, making this model the more acceptable of the two MC-SYM models. The 93−211 model has a 90° angle between the tRNAs, with the P site ACCA acceptor stem coming across the top of the D stem of the A site tRNA. The one unusual feature of these models compared with previous models (21, 22, 23, 24) is the P site acceptor stem crosses over the A site acceptor stem or T stem.

DISCUSSION

The prevalence of S models and the lack of a viable R model from the MC-SYM search process was rather surprising. Lim *et al.* (21) had concluded that the R model explained many of the crosslinks observed between the tRNA/mRNA complex and ribosomal proteins/RNA (21, and references therein). The proximity of A and P site tRNAs to various ribosomal proteins implied that the R model was the correct orientation. The exit of the mRNA was also used as an argument in favor of the R model. Much of the data used to draw the conclusion in favor of the R model is not applicable in the present study, because we are examining the distances within the mRNA−tRNA complex, not between the complex and the ribosome.

The FRET data used in constructing our MC-SYM models was considered insufficient by Lim *et al.* to distinguish whether the R or S model was correct. The crosslink from the A site tRNA to C1400 used as a constraint in the MC-SYM search was not considered by Lim *et al.* to provide enough information about the relative positions of the A and P site tRNAs. To be acceptable, the R or S models must agree with these data. Although the MC-SYM search process used in our study may be limited by the number or set of nucleotide conformations, the search results do indicate an overall conformation for the two tRNAs consistent with the FRET data and the two crosslinks. An examination of the A site tRNA crosslink to C1400 gives some distance and orientation implications for the arrangement of the A site tRNA relative to the P site tRNA. In addition, information regarding the replacement of conserved pyrimidines in the P site tRNA with purines (16) gives some indication of the orientation of the tRNAs in the ribosome. The following observations regarding the experimental data implicates the S model as the better of the two models in explaining these experimental results.

A comparison of the R and S models is necessary given the FRET data and crosslinks. However, comparing the MC-SYM models, built up from individual nucleotides, to the one available R model from Lim *et al.*, which was constructed from tRNA crystal structure, is inappropriate because the method of construction and emphasis on constraints differs. It is more appropriate to make comparisons among available models that were constructed in the same manner. Thus a comparison of FRET and crosslink distances in the Lim *et al.* (21) R and S model was made, since no R conformations were produced by MC-SYM.

The distances in table 4 demonstrate the weaknesses and strengths of each type of model in explaining the FRET measurements. Table 4 shows the problem of incorporating distance constraint from the A site nucleotide 37 to P site nucleotides 16 and 17 into the S type model produced by our

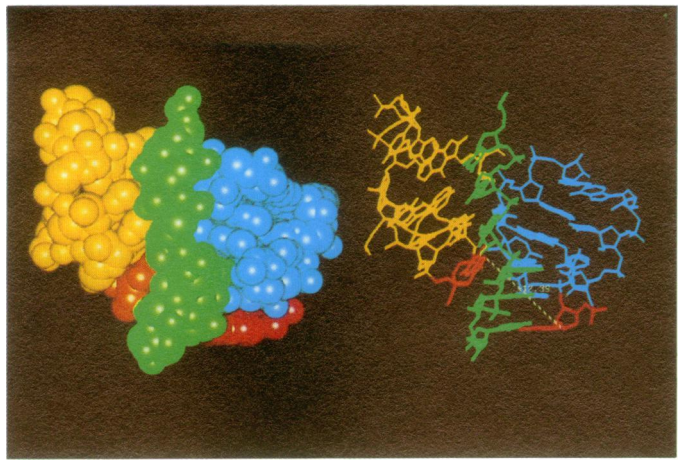

Figure 4. (left) A van der Waals representation of the Lim *et al.* (21) R model anticodon loop and mRNA region. The P site is yellow, the A site is blue, the message is green with the 5′ end up, and nucleotide 34 on each tRNA is highlighted in orange (P site) and red (A site). There is a lack of space for C1400 to stack next to P site nucleotide 34 (orange). (right) Stick representation of the R model anticodon loop and mRNA region. The distance between nucleotide 34 N7 on each tRNA is ~12 angstroms. The C1400 of the 16S rRNA would need to be between nucleotide 34 of the P site (orange) and the message.

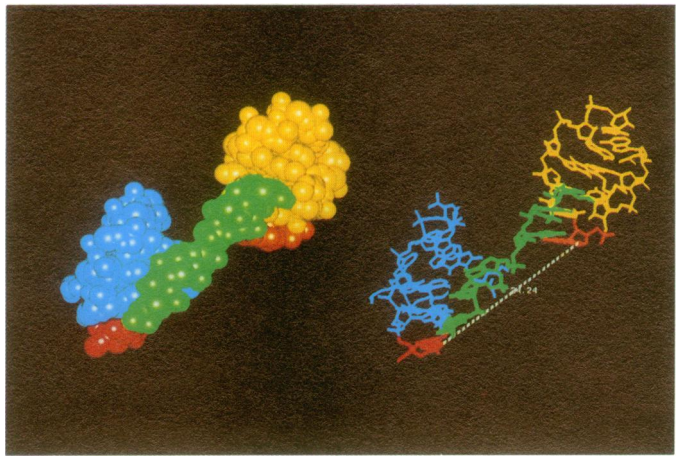

Figure 5. (left) A van der Waals representation of the Lim *et al.* (21) S model anticodon loop and mRNA region. The P site is yellow, the A site is blue, the message is green with the 5′ end to the right, and nucleotide 34 on each tRNA is highlighted in orange (P site) and red (A site). Space available for C1400 to stack beneath the P site nucleotide 34 (orange) is available. (right) Stick representation of the S model anticodon loop and mRNA region. The distance between nucleotide 34 N7 on each tRNA is ~24 angstroms. The C1400 of the 16S rRNA could easily stack beneath the P site nucleotide 34 (orange) without interference from the message. The photoactivatable probe used to crosslink the A site tRNA to C1400 would extend along the direction of the dashed line drawn between the two residues.

MC-SYM search procedure. However, one striking feature of the S model is its ability to accommodate constraints related to the anticodon loop. In the R model the nucleotide 37 to nucleotide 37 distance is rather small at 13 Å. In the S model the nucleotide 37 to nucleotide 37 distance is 22 Å, which is in better agreement with the Paulsen *et al.* data (14). Also, a measure of the distance from nucleotide 34 of the P site to nucleotide 34 of the A site

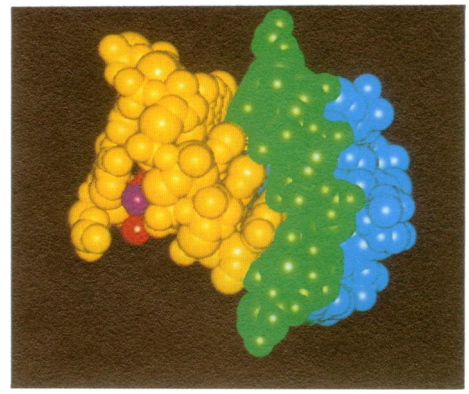

Figure 6. Space filling model of the anticodon loop and mRNA from the Lim *et al.* (21) R model. The P site tRNA anticodon loop is yellow, the A site tRNA anticodon loop is blue, the mRNA is green with the 5′ end up. The red nucleotide is U33, and the purple atom is the position of the uridine carbonyl oxygen O4 and represents the position of O6 in guanidine and N6 in adenosine when substituted for nucleoetide 33. The direction of the protruding atom is away from the A site and no direct interaction with A site tRNA would occur in the R model.

in the Lim *et al.* R model yields a distance of approximately 12 Å (atom N7 to atom N7) as seen in figure 4. In the Lim *et al.* S model the corresponding distance shown is approximately 24 Å (figure 5), which is in good agreement with the crosslinking data (10, 11).

The ability of P site $tRNA^{Val}$ U34 to photodimerize with C1400 implies a stacking arrangement for these two bases. In the Lim *et al.* R model it is difficult to place C1400 in a stacked position against P-site tRNA residue 34 due to steric hindrance (figure 4). On the other hand, it is no problem to stack C1400 below the P-site tRNA residue 34 in the S model (figure 5).

The chemical crosslink information (8,9,10,11) also gives some implication of the type of arrangement in the decoding region of the ribosome. The ability of the A site tRNA to crosslink to C1400 via the 23–24 angstrom probe implies C1400 is exposed and at the correct orientation for the crosslink to occur. In the R model C1400 would be partially or fully buried between the two tRNAs (figure 4). However, in the S model C1400 would be highly exposed as indicated by the experimental data (figure 5). The crosslink from A site U34 to C1400 also implies an orientation that would predominantly give crosslinks to C1400. In the R model the orientation of A site tRNA U34 atom C5 and the attached photoactivatable probe would be away from the P site tRNA and C1400, implying the most prevalent crosslinks would likely be away from the P site. In the S model atom C5 of the A site residue U34 faces toward the P site and in the putative location of C1400, which is a better orientation in the light of the experimentally observed crosslink (10, 11). In the R model the orientation and attachment of the probe to the A site tRNA requires a special bending of the probe around or under the A site tRNA to crosslink to C1400. The S model does not necessitate any special bending of the probe.

The capacity to crosslink both the P and A site tRNAs simultaneously to C1400 would also help determine whether the R or S model is correct. If tRNAs can bind to the A and P site in the ribosome and the tRNAs are able to crosslink to C1400 simultaneously (12), the R model is definitely less feasible than the S due to the steric, distance, and orientation evidence listed

above. All of the information to date regarding the two crosslinks to C1400 indicate the S model as the best fit for the data.

The data from Smith and Yarus (16) argues for some contact between residue 33 in the P site tRNA and the A site tRNA. Such an interaction is not present in the MC-SYM created models nor in the S models from Lim *et al.* (21). The anticodon region in the Lim *et al.* R model, shown in figure 6 with nucleotide 33 highlighted, also does not account for the interaction. However, the S models created by Smith and Yarus (16) and by Prabahakaran and Harvey (24) are able to demonstrate the interaction. In Smith and Yarus, substitution of G or A for U33 in the P site tRNA anticodon loop led to a decrease in stop codon suppression at the A site. Substituting adenine for U33 in the P site provided the greatest amount of suppression inhibition. As pointed out by Smith and Yarus (16), steric hindrance cannot be the only factor involved, since the insertion of A and G do not give a similar perturbation of the system. If the substituted A and G bases maintain an *anti* base conformation in the tRNA, the orientation of the carbonyl oxygen at position six on guanine and position four on uracil would have the same orientation. Thus the differences seen in replacing U33 with G is primarily steric. The change from U to A substitutes an amine for the carbonyl oxygen, and hence changes the charge of the protruding group as well as the steric makeup of the molecule.

Since base substitutions at the P site prevent the *binding* of tRNA in the A site (16), the route that the tRNA takes as it enters the A site may be blocked by the electrostatic and steric effects from the base substitutions. The A site tRNA would be prevented from immediately binding to the codon, allowing the release factors time to bind to the stop codon and terminate translation as proposed by Smith and Yarus (16). This scenario may explain why there is no interaction seen between the A site U33 and P site tRNA in the MC-SYM models; the interaction would occur before the tRNA entering the A site pairs with its codon. In the R model nucleotide 33 of the P site tRNA would project away from the A site having no direct effect on the tRNA entering the A site (figure 6). In the S model the nucleotides also do not directly face the A site but do project more toward the A site than in the R model, providing electrostatic and steric effects. One S model showing the interaction between nucleotide 33 in the P site tRNA with the A site tRNA is the Prabahakaran and Harvey (24) model. If close contacts are occurring, some crosslink between the tRNAs might occur in this anticodon region if the appropriate nucleotide analogs are substituted for P site nucleotides 32 and 33 . To date no direct crosslink between A and P site tRNAs have been found (12).

CONCLUSION

Models of two tRNAs as positioned in the ribosome were constructed using MC-SYM. Surprisingly the resulting structures were exclusively of the S variety. The Lim *et al.* (21) modeling study concluded that the R conformation was best at explaining crosslinks from tRNA/mRNA to the ribosome. In that study the proximity of the A site tRNA to the proteins in the L7/L12 stalk and the orientation of the mRNA relative to the 30S subunit were used as arguments in favor of the R orientation. However, information regarding the distances between tRNAs in the ribosome must also be consistent with the model, and we find that the R models do not fully satisfy constraints derived from distances determined by fluorescence energy transfer and crosslinking. Detailed nucleotide conformational and structural aspects of two crosslinks from U34 of both A and P site tRNA directly to C1400 of the 16S rRNA imply an S configuration in the ribosome. Further, the two crosslinks appear to occur simultaneously in the ribosome, and such a result would almost necessitate an S conformation. In addition to fluorescence data and crosslinks, information regarding base substitution in the anticodon loop is also better explained by the S model. Given the current information regarding two tRNAs as positioned in the ribosome, the S model answers all experimental data regarding the direct interaction of the anticodon loops better than the R model. In support of this conclusion, while this paper was in review additional crosslinks between mRNA and the ribosome (29) and between the tRNA anticodon loops and the ribosome (30) have led Brimacombe and coworkers to favor the S model.

ACKNOWLEDGMENTS

We thank Dr Richard Brimacombe and Dr Michael R.McBride for excellent discussions and constructive criticism. This work was supported by National Science Foundation grant DMB-90-05767.

REFERENCES

1. Rheinberger, H.-J., Sternbach, H. and Nierhaus, K.H. (1981) Proc. Natl. Acad. Sci. U.S.A., 78, 5310–5314.
2. Nierhaus, K.H. (1990) Biochemistry, 29, 4997–5008.
3. Nierhaus, K.H. (1993) Mol. Microbiol., 9, 661–669.
4. Fairclough, R.H., Cantor, C.R., Wintermeyer, W. and Zachau, H.G. (1979) J. Mol. Biol., 132, 557–573.
5. Odom, O.W., Craig, B.B. and Hardesty, B.A. (1978) Biopolymers, 17, 2909–2931.
6. Matzke, A.J.M., Barta, A. and Kuechler, E. (1980) Proc. Natl. Acad. Sci. USA, 77, 5110–5114.
7. Steiner, G., Lührmann, R. and Kuechler, E. (1984) Nucleic Acids Res., 12, 8181–8191.
8. Prince, J.B., Taylor, B.H., Thurlow, D.L., Ofengand, J. and Zimmermann, R.A. (1982) Proc. Natl. Acad. Sci. USA, 79, 5450–5454.
9. Ofengand, J., Liou, R., Kohut, J. III, Schwartz, I. and Zimmermann, R.A. (1979) Biochemistry, 79, 4322–4332.
10. Gornicki, P., Ciesiolka, J. and Ofengand, J. (1985) Biochemistry, 24, 4924–4930.
11. Ciesiolka, J., Gornicki, P. and Ofengand, J. (1985) Biochemistry, 24, 4931–4938.
12. Ofengand, J., Ciesiolka, J. and Nurse, K. (1986) In van Knippenberg, P.H. and Hilbers, C.W. (eds.) Structure and Dynamics of RNA. Plenum Publishing Corporation, New York, pp. 273–287.
13. Ofengand, J., Ciesiolka, J., Denman, R. and Nurse, K. (1986) In Hardesty, B. and Hilbers, C.W. (eds.) Structure, Function, and Genetics of Ribosomes. Springer-Verlag New York Inc., New York, New York, pp. 473–494.
14. Paulsen, H., Robertson, J.M. and Wintermeyer, W. (1983) J. Mol. Biol., 167, 411–426.
15. Johnson, A.E., Adkins, H.J., Matthews, E.A. and Cantor, C.R. (1982) J. Mol. Biol., 156, 113–140.
16. Smith, D. and Yarus, M. (1989) Proc. Natl. Acad. Sci. USA, 86, 4397–4401.
17. Lustig, F., Boren, T., Claesson, C., Simonsson, C., Barciszewska, M. and Lagerkvist, U. (1993) Proc. Natl. Acad. Sci. USA, 90, 3343–3347.
18. Fuller, W. and Hodgson, A. (1967) Nature, 215, 817–821.
19. Woese, C. (1970) Nature, 226, 817–820.
20. Rich, A. (1974) In Nomura, M., Tissieres, A. and Lengyel, P. (eds.) Ribosomes. Cold Spring Harbor Laboratory, New York, pp. 871–884.
21. Lim, V., Venclovas, C., Spirin, A., Brimacombe, R. and Muller, F. (1992) Nucleic Acids Res., 20, 2627–2637.
22. Sundaralingam, M., Brennan, T., Yathrinda, N. and Ichikawa, T. (1988) In Sundaralingam, M. and Rao, S.T. (eds.) Structure and Conformation of Nucleic Acids and Protein–Nucleic Acid Interactions. University Park Press, Baltimore, pp. 101–115.
23. MacDonald, J.J. and Rein, R. (1987) J. Biomol. Struct. Dyn., 4, 729–744.

24. Prabahakaran, M. and Harvey, S.C. (1989) J. Biomol. Struct. Dyn., 7, 167–177.
25. Major, F., Turcotte, M., Gautheret, D., Lapalme, G., Fillion, E. and Cedergren, R. (1991) Science, 253, 1255–1260.
26. Major, F., Gautheret, D. and Cedergren, R. (1993) Proc. Natl. Acad. Sci. USA, 90, 9408–9412.
27. Gautheret, D., Major, F. and Cedergren, R. (1993) J. Mol. Biol., 229, 1049–1064.
28. Brown, R.S., Dewan, J.C. and Klug, A. (1986) Biochemistry, 24, 4785–4801.
29. Rinke-Appel, J., Jünke, N., Brimacombe, R., Laverick, I., Dokudovskaya, S., Dontsova, O., and Bogdanov, A., Nucleic Acids Res. (in press.)
30. Döring, R., Mitchell, P., Osswald, M., Bochkariov, D., and Brimacombe, R. (1994) EMBO J., 13, 2677–2685.
31. Saenger, W. (1984) In Cantor, C.R. (ed.) Principles of Nucleic Acid Structure. Springer-Verlag New York Inc., New York, New York.